

Evaluation of GPS L5, Galileo E1 and Galileo E5a Performance in Flight Trials for Multi Frequency Multi Constellation GBAS

M.-S. Circiu*, M. Felux*, B. Belabbas*, M. Meurer*⁺, Jiyun Lee[†], Minchan Kim[‡], Sam Pullen[°]

* *Institute of Communications and Navigation, German Aerospace Center (DLR), German Aerospace Center (DLR)*

⁺ *Chair of Navigation, RWTH Aachen University, Germany*

[‡] *Korea Advanced Institute of Science and Technology*

[°] *Stanford University*

ABSTRACT

This paper presents a noise and multipath performance analysis of the new signals broadcast by the Block IIF GPS satellites on L5 and Galileo satellites on E1 and E5a using airborne flight data. Improved performance has been previously observed using ground measurement and is now validated using data from different flight tests. This is especially true for GPS L5 and Galileo E5a. However, on the airborne side, the performance of Galileo E1 signal is closer to that of GPS L1. The impact of different parameters on the airborne multipath, including receiver correlator spacing, airframe structure, ground influence, and smoothing time, are investigated and discussed.

1. INTRODUCTION

For civil aviation navigation systems, very stringent requirements concerning accuracy, continuity, availability and especially integrity have to be met. The aim of the Ground Based Augmentation System (GBAS), a development of local-area differential GNSS, is to provide precision approach guidance meeting all of these requirements under low-visibility conditions. GBAS ground stations supporting CAT I precision approaches (so-called GBAS Approach Service Type C, or GAST C) are already in service, while systems supporting CAT II/III approaches (termed GAST D) are under development and are expected to become operational in the next several years. The current GBAS architecture for both GAST C and D is based on the use of GPS satellites and single frequency L1 C/A code only. In order to fulfill the GAST C and GAST D requirements, integrity monitors are necessary to detect and exclude unsafe measurements from the navigation solution. However, these monitors have a negative impact on continuity and availability of the service.

More and more Galileo and GPS Block IIF satellites are being launched, providing additional satellites broadcasting a second frequency in the ARNS band (E5a/L5). The use of signals in different frequency bands and from multiple GNSS constellations has the potential to significantly improve GBAS performance compared to GAST C and GAST D by adding geometric diversity and allowing much better estimation and removal of errors induced by the ionosphere.

Multipath and noise are significant contributors to the residual differential error in GBAS. Multipath errors affect both the ground and the airborne receivers. The ground facility uses antennas specifically designed and sited to eliminate most of the multipath effects. The residual uncertainty in the transmitted corrections attributed to noise and multipath is determined and broadcast by the ground station (σ_{pr_gnd}). Airborne multipath may occur due to the airframe or due to ground reflections during landing. It represents a potentially large source of error and drives the overall pseudorange residual uncertainty and thus the protection level which bounds the residual position errors.

Models based upon carrier-smoothed GPS L1 C/A code measurements were defined to classify the airborne receiver and antenna using an Airborne Accuracy Designator (AAD) and specified multipath and error models for each AAD class [9]. Unlike the ground station, the residual uncertainty attributed to the airborne multipath and noise (σ_{pr_air}) is computed based on this standardized error model. In our previous work [2][3], we presented the first evaluation of new signal performance (GPS L5, Galileo E1 and E5) using measurements from our GBAS ground system in Braunschweig. The results for the limited number of satellites available to be evaluated indicated that the noise and multipath influence on the new signals is significantly reduced and the ranging performance thus improved.

After this evaluation of ground data, the step addressed in this paper is evaluation of data from flight trails to determine if similar improvements can be observed in airborne multipath and noise characteristics. This paper presents the evaluation of the airborne multipath and noise for GPS L5 and Galileo E1 and E5a signals. Measurements from multiple flight tests using different aircraft test platforms were collected to validate the performance of the new signals. The DLR research aircraft, the Dornier 228 and the Airbus A320 were used in these flight trials. In addition, data from flight experiments using KAIST's Unmanned Aerial Vehicle (UAV) are considered for comparison and determination of ground reflections. Dual frequency GPS L1 and GPS L5 as well as Galileo E1 and Galileo E5a measurements are recorded by the receivers onboard each test platform. Unlike the evaluation of the ground data, in which σ_{pr_gnd} was estimated based on the B-value method as

described in ED-114A, Section 5.4.4, the airborne multipath is estimated using the divergence-free code minus carrier method described below [7].

This work supports the definition of future multi-frequency multi-constellation airborne multipath models represented by the parameter σ_{pr_air} which has a large influence in the protection level calculation and thus on the overall performance. The most important contributors to σ_{pr_air} are the receiver parameters, the airframe, the ground influence and the smoothing filter constant. These aspects are presented in detail in Sections 6-9, after a short discussion on multipath estimation in Sections 2 and 3, a review of the current models in Section 4 and a review of our data collections and flight trials in Section 5.

2. MULTIPATH ESTIMATION

As a first step, we present an assessment of noise and multipath on the different GNSS signals. The method we apply to estimate the multipath in this work is differencing the code and carrier-phase measurements (CMC). Carrier phase is very precise, and the multipath error on carrier is a couple of orders of magnitude smaller than the code multipath and thus negligible in the context of this work. Expressions describing code and carrier phase measurements are given in equations (1) and (2), respectively.

$$\rho_i = r + c(dt_u - dt^s) + T + I_i + MP_{\rho,i} + \varepsilon_{\rho,i} \quad (1)$$

$$\phi_i = r + c(dt_u - dt^s) + T - I_i + N_i\lambda_i + MP_{\phi,i} + \varepsilon_{\phi,i} \quad (2)$$

where r is the true geometric range from user to the satellite, I_i is the ionospheric delay for frequency i , T is the tropospheric delay, dt_u is the receiver clock bias, dt^s is the bias in the satellite clock bias, $MP_{\rho,i}$ and $\varepsilon_{\rho,i}$ are the code multipath and thermal noise on frequency i , $MP_{\phi,i}$ and $\varepsilon_{\phi,i}$ are the phase multipath and thermal noise on frequency i , and N_i is the integer ambiguity on frequency i .

Differencing the code and the carrier-phase measurements, the new observable contains twice the ionospheric delay, the integer ambiguity, and the code multipath and noise, and it is described in equation (3).

$$\rho_i - \phi_i = 2I_i + N_i\lambda_i + MP_{\rho,i} + \varepsilon_{\rho,i} \quad (3)$$

Note that if there are no cycle slips, the integer ambiguity remains constant.

With dual-frequency measurements, it is possible to remove the ionospheric delay. Using the first-order relationship of the ionospheric delay difference between two frequencies i and j $I_j = f_i^2/f_j^2 I_i$, the ionospheric error can be written as:

$$I_i = \frac{f_j^2}{f_i^2 - f_j^2} (\phi_i - \phi_j) - \frac{f_j^2}{f_i^2 - f_j^2} (N_i\lambda_i - N_j\lambda_j) \quad (4)$$

where f_i and f_j are the center frequencies of the respective ranging signals.

Replacing the ionospheric delay in equation (3) with the expression from equation (4), we obtain the multipath and thermal noise estimation:

$$MP_{\rho,i} + \varepsilon_{\rho,i} = \rho_i - \phi_i - 2 \frac{f_j^2}{f_i^2 - f_j^2} (\phi_i - \phi_j) + b \quad (5)$$

The bias, b , containing the integer ambiguity combination is removed by subtracting the mean over a continuous pass for each satellite, as the noise and multipath are expected to be zero mean.

3. AIRBORNE MULTIPATH FOR GBAS

The expression given in equation (5) gives an estimate of the raw code noise and multipath on a measurement. However, in the GBAS implementation, carrier smoothing is performed to reduce high frequency noise and multipath. The models for σ_{pr_air} are thus defined to overbound the residual airborne receiver noise after carrier smoothing. Smoothed results are obtained using a low-pass filter as described in DO-253C [12], which can be formulated as

$$\widehat{MP}_{\rho,i}(k)\widehat{\varepsilon}_{\rho,i}(k) = \alpha \left(MP_{\rho,i}(k) + \varepsilon_{\rho,i}(k) \right) + (1 - \alpha) \left(\widehat{MP}_{\rho,i}(k-1) + \widehat{\varepsilon}_{\rho,i}(k-1) \right) \quad (6)$$

where the expressions with a hat indicate smoothed parameters, α represents the filter time constant, and k represents the epoch count (each epoch lasts 0.5 seconds in GBAS).

As σ_{pr_air} is elevation dependent, the collected measurements are first sorted according to the corresponding satellite elevation and are grouped into bins (1° bin size for elevations below 30° , 2° for elevations between 30° and 50° , and 5° for elevations above 50°). Assuming a zero mean of the effect of noise and multipath, the standard deviation for all values in each bin is computed. The current GPS L1 C/A code models include the contributions of thermal noise and multipath separately. In this work only the total σ_{pr_air} is evaluated, as it is difficult to distinguish between the two components. However, the multipath is correlated in time and will remain predominant after smoothing, while the noise is uncorrelated and will be smoothed out almost completely.

Unlike atmospheric effects, multipath is a local effect and is highly dependent on the aircraft structure. Thus, residual errors in airborne measurements depend on the elevation of the satellite relative to the airframe. In the current requirements, the elevation angle only refers to the elevation of the satellite relative to the horizon. This is

justified by assuming that the approach will mostly be flown with wings level. This assumption is true for ILS-like straight-in approaches. However, it should be reconsidered for advanced approach procedures, which may include curved approaches, where the full benefits of GBAS will be exploited in the future.

Roll, pitch and heading information from the basic aircraft instrumentation are used to translate satellite coordinates into the aircraft body frame as described in equation (7). Elevation and azimuth angles of the satellite in the aircraft body frame (X_{BF}, Y_{BF}, Z_{BF}) are computed using

$$\begin{pmatrix} X_{BF} \\ Y_{BF} \\ Z_{BF} \end{pmatrix} = \begin{bmatrix} 1 & 0 & 0 \\ 0 & \cos\phi & \sin\phi \\ 0 & -\sin\phi & \cos\phi \end{bmatrix} * \begin{bmatrix} \cos\theta & 0 & -\sin\theta \\ 0 & 1 & 0 \\ \sin\theta & 0 & \cos\theta \end{bmatrix} * \begin{bmatrix} \cos\Psi & \sin\Psi & 0 \\ -\sin\Psi & \cos\Psi & 0 \\ 0 & 0 & 1 \end{bmatrix} \quad (7)$$

$$elevation = \arctan\left(\frac{Z_{BF}}{\sqrt{X_{BF}^2 + Y_{BF}^2}}\right) \quad (8)$$

$$azimuth = \arctan\left(\frac{X_{BF}}{\sqrt{X_{BF}^2 + Y_{BF}^2}}\right)$$

where Ψ is the heading angle, θ is the pitch angle, and ϕ is the roll angle. The results derived from our measurements are all sorted into elevation bins according to the elevation of the satellite with respect to the airframe.

4. CURRENT AIRBORNE MULTIPATH MODELS

Previous work has assessed the contribution of airborne receiver thermal noise and airframe multipath to the airborne accuracy allocation for GPS L1 C/A code [1][10][11]. It was agreed that one standard model should be developed for airborne multipath and be included in the σ_{pr_air} term. The aim was to define a single model for all aircraft types in order to avoid individual certifications for each type of aircraft. Even though the studies showed that the multipath error does depend on the specific airframe, the distributions are similar enough to be bounded by a single model [1].

The airborne multipath model was proposed in [1] and validated in [10][11] through a joint effort between the FAA, Boeing and Honeywell with periodic reviews from RTCA and ICAO. The data was collected using different models of Boeing planes and different receiver types. The adopted multipath model as presented in DO-253 ([12]) is described by

$$\sigma_m = 0.13 + 0.53 * e^{-\frac{\theta}{10}} \quad (9)$$

where θ is the elevation angle in degrees. In addition, the standards include the Airborne Accuracy Designator

(AAD) performance for receiver thermal noise [12] [9]. Two curves were defined, the so-called AAD-A and AAD-B models, described by:

$$\sigma_n(\theta) = 0.15 + 0.43 e^{-\frac{\theta}{6.9}}, \quad \text{for AAD - A} \quad (10)$$

$$\sigma_n(\theta) = 0.11 + 0.13 e^{-\frac{\theta}{4}}, \quad \text{for AAD - B} \quad (11)$$

All of these models were derived for 100-second smoothed code measurements, and the total σ_{pr_air} is the root sum square of the multipath and noise components as a function of satellite elevation:

$$\sigma_{pr_air}(\theta) = \sqrt{\sigma_m^2(\theta) + \sigma_n^2(\theta)} \quad (12)$$

In previous research, we have shown that the new signals broadcast on GPS L5 and Galileo E1 and E5a have better performance in terms of lower multipath and noise [3]. Until now, only data from ground stations has been analyzed. Now having available data from flight tests, the new signals' performance on the airborne side is evaluated.

5. DATA COLLECTION

For data collection, different vehicles were used. Most of the data was collected with DLR's Airbus A320. In order to collect as much data as possible, a Javad Delta TRE3 receiver is now permanently installed in the A320. This receiver tracks GPS and Galileo signals on L1, L2 and L5 at a rate of 20 Hz. During the flight tests, we used two different correlator spacings in the receiver in order to evaluate the influence of different receiver parameters on airborne performance. The airborne antenna installed on the aircraft is an active Antcom multiband antenna. Figure 1 shows the aircraft and the location of the GNSS antenna.



Figure 1 - DLR's Airbus A320 research aircraft "ATRA". The location of the experimental GNSS antenna is marked by the red arrow

Data from each test flight of the aircraft was collected and analyzed and thus contributed to modelling the airborne performance with increasing confidence. The data used for this study was collected during 18 test flights in June and July 2015. These were mostly local flights across northern Germany along with one flight from Braunschweig to Paris and back. We analyzed a total of

about 40 hours of flight data. As the aircraft was flying for several different experiments, the visibility of GPS Block IIF and Galileo satellites varied.

In March 2015, a number of flights were conducted with DLR's Dornier DO-228 (Figure 2), a twin-propeller aircraft significantly smaller than the A320. The plane was equipped with a Javad Delta G3TH receiver with the same functions and parameters as in the Airbus. At that time, the firmware only supported a very narrow correlator of 0.015 chips. Thus, only data with that spacing were available for evaluation. The scope of the March campaign was to collect new GPS IIF and Galileo signals in order to evaluate the noise and multipath and to confirm the improvements observed in the previous ground-system evaluations [2][3]. The flight schedule was chosen during times of good visibility of GPS Block IIF and Galileo satellites. During the flight campaign, 8 Block IIF GPS and 3 Galileo satellites were available and healthy. Dual-frequency code and carrier-phase measurements on L1 (E1) and L5 (E5a) were recorded and post processed to assess the multipath error. Figure 2 shows the aircraft and the location of the GNSS antenna.



Figure 2 - DLR's Dornier-228 research aircraft "D-CODE" (top). The location of the experimental GNSS antenna is shown on the bottom figure

As the amount of data collected to date is limited, all results should be considered to be preliminary and have to be validated when more data is available. However, they do give a good indication as to what kind of performance can be expected.

During flight, airborne multipath only results from reflections from the airframe. However, as the aircraft approaches the ground and rolls out on the runway, additional multipath from ground reflections impacts the signals. In order to study and characterize the effects of multipath due to ground reflections, KAIST collected GNSS data in Cheongju and Daejeon, South Korea in August 2015. The primary objective of the data collection was to assess and compare the performance of Galileo E1 and GPS L1 signals under different multipath conditions at different altitudes near the ground. Data were collected at three different altitudes of 0, 10, and 20 meters.

The 20-meter data set was collected using a UAV which was set to hover at the designated altitude using its built-in autopilot functions. Figure 3 shows the octocopter platform used for this flight test [8]. It has a diameter of 135 cm, height of 45 cm, and weighs 5.26 kg when all of the equipment is loaded. The onboard GNSS equipment consists of a NovAtel GPS-703-GGG antenna and a NovAtel FlexPak-6 receiver. This receiver has a bandwidth of 15 MHz and a 0.1-chip correlator spacing for L1/E1 signals. These receiver and antenna characteristics were consistent for all three data collections at varying altitudes. Due to the structural characteristics of the UAV airframe, the amount of multipath from reflections on the UAV itself is likely to be very small. Consequently, the majority of the multipath in the data collected from the UAV can be considered to be due to ground reflections. The data used for this analysis was collected over the course of 10 flight tests for a total of 30 hours.

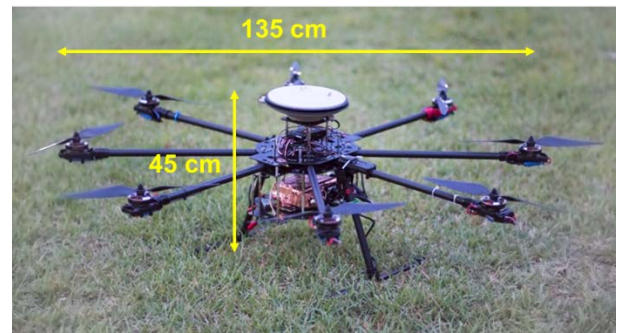


Figure 3 - Multi-copter UAV platform for flight test

The 10-meter data set was collected using one of the antenna mounts of the KAIST Local Area Differential GNSS Integrity Monitor Test-bed (IMT). The same antenna and receiver used for the UAV flight trials were installed in the corner of the roof of the seven-storey tall KAIST Mechanical Engineering Building using a 5-meter steel rod mount. As the majority of the multipath is from the surface of the rooftop and the surrounding buildings in the vicinity of the antenna, we believe that this setup is similar to gathering data from a hovering UAV at an altitude of about 10 meters from the ground.

The 0-meter data set was collected from the UAV while located on the surface of the ground, with no severe obstacles in the vicinity (within a radius of several hundred meters). This is similar to typical airport conditions (flight test was taken near Cheongju airport).

6. RESULTS FROM FLIGHT TESTS

The initial analysis of airborne multipath and noise is performed using the data collected from the DLR's Airbus, as it is representative of a commercial airplane. The receiver has a 23 MHz bandwidth, thus a correlation peak sampling values of 0.1 chips value were chosen for L1/E1 signals and 1.0 chip for L5/E5a signals. The impact of the correlator spacing will be detailed in the

next section. Even though the amount of data is limited, it gives a first idea on what to expect as nominal airborne multipath performance.

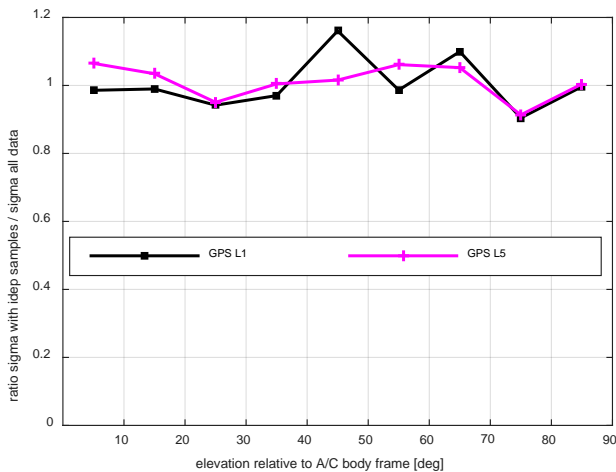


Figure 4 - Ratios of σ_{pr_air} function of elevation in aircraft body frame using independent samples and the total amount of data

The standard deviation of the airborne multipath and noise, or σ_{pr_air} , is computed by sorting independent measurement samples into elevation bins. In order to insure the use of independent samples, a sample is collected from the data set at intervals corresponding to every 2 smoothing time constants. However, the airborne multipath itself is expected to be only slightly correlated in time. This can be seen in the curves in Figure 4, where the ratios between the standard deviations computed based on the whole set of data in each bin and independent samples (one sample every 200 seconds) for GPS L1 and L5 signals are shown.

In general, the same behavior characteristics have been observed for all signals. Thus, in all further evaluations, the total amount of data collected is combined together in the results. Due to the limited amount of data available despite this, a satellite elevation bin width of 10 degrees was chosen in this work.

Figure 5 shows the standard deviations of smoothed code noise and multipath with the corresponding 95% confidence intervals for each elevation bin. The 95% confidence intervals are computed as $\left[\sqrt{\frac{(n-1)s^2}{\chi^2_{\alpha/2, n-1}}}, \sqrt{\frac{(n-1)s^2}{\chi^2_{1-\alpha/2, n-1}}} \right]$, where s is the sample variance and n the number of independent samples in each bin. Data was smoothed using a 100-second smoothing time constant. As discussed above, in order to insure the use of independent samples, a value every 200 seconds was selected from the data set.

As observed on the ground, the new signals have improved performance in terms of noise and multipath reduction. This is especially true for the GPS L5 and Galileo E5a signals that have a ten times higher chipping

rate than the L1 and E1 signals. However, on the airborne side, unlike on the ground side, the performance of the Galileo E1 signal is closer to that of GPS L1. This can be explained by the fact that the improvement of the BOC modulation is more pronounced for long range multipath, which is typical for the ground environment of stationary receivers and antennas. In an operational GBAS system, this effect will however be not as strong thanks to the use of multipath limiting antennas and carefully prepared reference antenna locations, which we did not have in our studies.

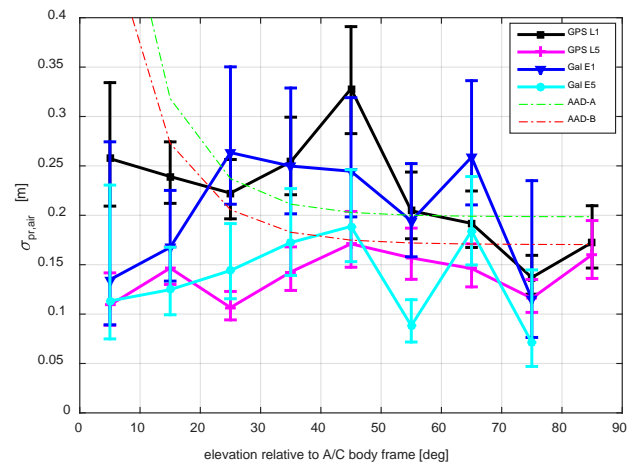


Figure 5 - Comparison of σ_{pr_air} for GPS L1 (black), GPS L5 (magenta) and Galileo E1 (blue) and E5a (cyan)

7. IMPACT OF THE CORRELATOR SPACING ON MULTIPATH

Two of the parameters that impact noise and multipath behavior of the receiver are the receiver bandwidth and correlator spacing. The current airborne specifications [12] define allowed regions for combinations of receiver bandwidth and early-minus-late correlator spacing as shown in Figure 6. From an integrity perspective, allowing a whole design space is an unfortunate situation, as the worst case combination has to be considered. This is, however, difficult to assess, as there are potentially an infinite number of points in the allowable region.

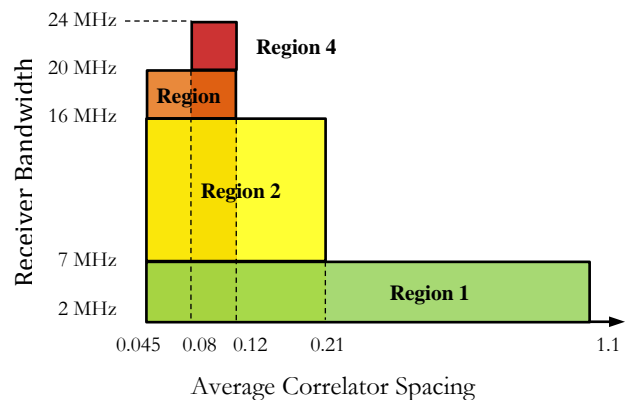


Figure 6 – Allowed E-L Discriminator Tracking of GPS satellites

In order to show the impact of different correlators on σ_{pr_air} , measurements from the same receiver used in the Airbus A320 with two different correlator spacing values are compared. The receiver (Javad Delta TRE3) has a bandwidth of 23 MHz, and the default correlator spacing is 0.015 chips for L1/E1 signals and 0.15 chips for L5/E5a signals. The narrow correlator for L1/E1 is outside the airborne specification, but it is a relevant value for very narrow correlator receivers. With customized firmware provided by Javad, the correlator was reset to 0.1 chips for L1/E1 and 1 chip for L5/E5a.

Figure 7 shows the comparison of the standard deviations of the code multipath and noise for GPS L1 and L5 for these two different values of the correlator spacing. For both signals there is a noticeable difference between the two cases. The difference is larger for GPS L1, especially at low elevations, than for GPS L5. The Galileo signals are not shown in the plot as only limited data was available. However, the first results show similar behavior as for the GPS signals.

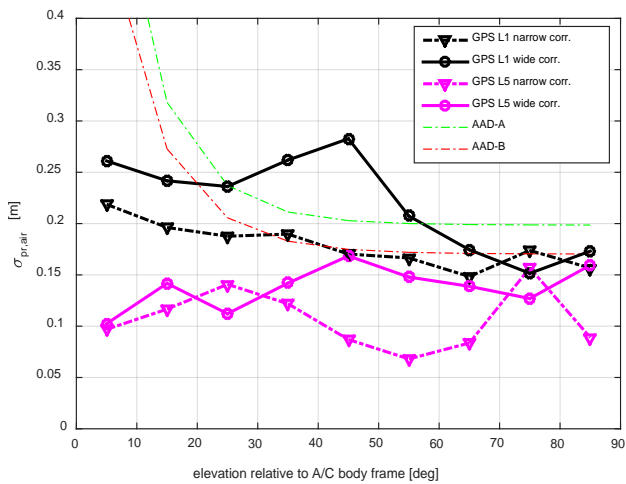


Figure 7 - Comparison of σ_{pr_air} using a narrow correlator (dashed lines) and a wide correlator (solid lines) for GPS L1 and GPS L5

Depending on the actual receiver design, σ_{pr_air} can differ significantly even on a single aircraft type. Another important aspect to consider for future multi frequency systems is that, for the L5 signals, a wider bandwidth will be required (above 20 MHz) to receive most of the transmitted signal. This will restrict the space for the correlator spacing for dual frequency receivers.

8. IMPACT OF THE AIRFRAME ON MULTIPATH

An important contributor to the airborne multipath is the shape of the airframe itself and the location of the GNSS antenna with respect to its reflecting surfaces. In order to evaluate the impact of different aircraft types and antenna locations, we collected measurements on two different aircraft of the DLR fleet, the DO-228 (named CODE) and the A320 (named ATRA). For this study, we used

measurements with the same correlator spacing (0.01 chips for L1/ E1 and 0.1 chips for L5/E5a) and receiver bandwidth in order to investigate only the impact of the airframe itself as distinct from the previously described influence of receiver correlator spacing.

Figure 8 shows a comparison of the standard deviations of the code multipath and noise for GPS L1 signals and Galileo E5a signals for the two different aircraft depending on satellite elevation. As previously described, the elevation of the satellites refers to the angle relative to the body frame, which is computed using the roll, pitch and heading information provided by the aircraft instrumentation.

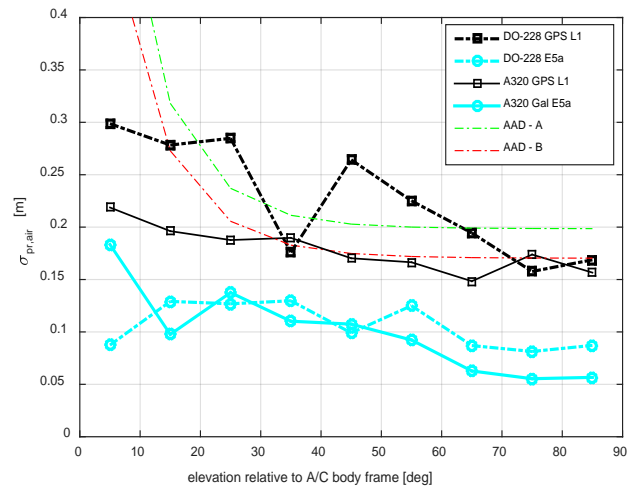


Figure 8 - σ_{pr_air} function of elevation for Dornier DO-228 (dashed lines) and Airbus A320 (solid lines) for GPS L1 (black) and Galileo E5a (cyan)

The solid lines in the above show the results obtained for the Airbus A320 while the dashed lines show the results for the Dornier DO-228. A possible explanation for these results might be the location of the DO-228 antenna (see Figure 2) close to the tailfin and other reflecting parts of the airframe. The measurements taken on the DO-228 aircraft show significantly higher multipath than those taken on the A320.

This effect is again much more pronounced for the GPS L1 signals than for the Galileo E5a signals. This was expected since the higher chipping rate on E5a, together with an increased transmitted signal power, yields significantly improved multipath rejection characteristics.

For clarity, only the results of GPS L1 and Galileo E5a signals were shown in Figure 8. The same effect of smaller differences between L5 measurements from the different aircraft types was also visible in the data not shown here.

9. SMOOTHING CONSTANT

After showing the impacts of receiver parameters and airframe geometry on airborne multipath and noise

characteristics, this section discusses possible consequences on the smoothing time constant required for the new signals. In a previous study based on measurements from the Braunschweig GBAS testbed, we observed that the new signals, GPS L5 and Galileo E1 and E5a, are less sensitive to the smoothing time constant [3]. For Galileo E1, a smoothing time constant longer than 60 seconds does not provide a significant improvement on the residual error, while for GPS L5 and E5a, there is already almost no additional error reduction for smoothing longer than 30 seconds. In the same manner, we evaluated effect of different smoothing times on airborne noise and multipath.

Figure 9 shows the $\sigma_{pr,air}$ curves for GPS L5 for the available Block IIF satellites compared with GPS L1 signals for smoothing time constants of 30, 60 and 100 seconds. Measurements collected from the A320 with 0.1 chip spacing for L1/ E1 and 1 chip spacing for L5/E5a were used for this evaluation. There is a noticeable difference between the different smoothing constants and the residual error is reduced as the filter constant increases. The effectiveness of carrier smoothing on

airborne error can be explained by the fact that the airborne measurements are heavily affected by fast changing short-range multipath, which is only slightly correlated in time. Uncorrelated noise-like behavior is very effectively reduced by the smoothing filter, and smoothing becomes more effective as the smoothing time constant increases. We also observe that the impact of extended smoothing on the L5 signals is significantly lower than that on L1. This effect was also expected, since the properties of the new signals show better performance in terms of multipath rejection. Thus, with lower multipath in the signals to begin with, the benefit of extended smoothing is not as large as with the L1 signals.

Figure 10 and Figure 11 show the smoothing filter performance for the Galileo signals. The same impact of smoothing filter duration is seen on E1 and E5a signals as for L1 and L5. As observed earlier for 100 seconds of smoothing (see Figure 5), Galileo E1 performance is close to GPS L1 for all smoothing time constants examined, while E5a shows improved performance similar with that observed from GPS L5 in Figure 9.

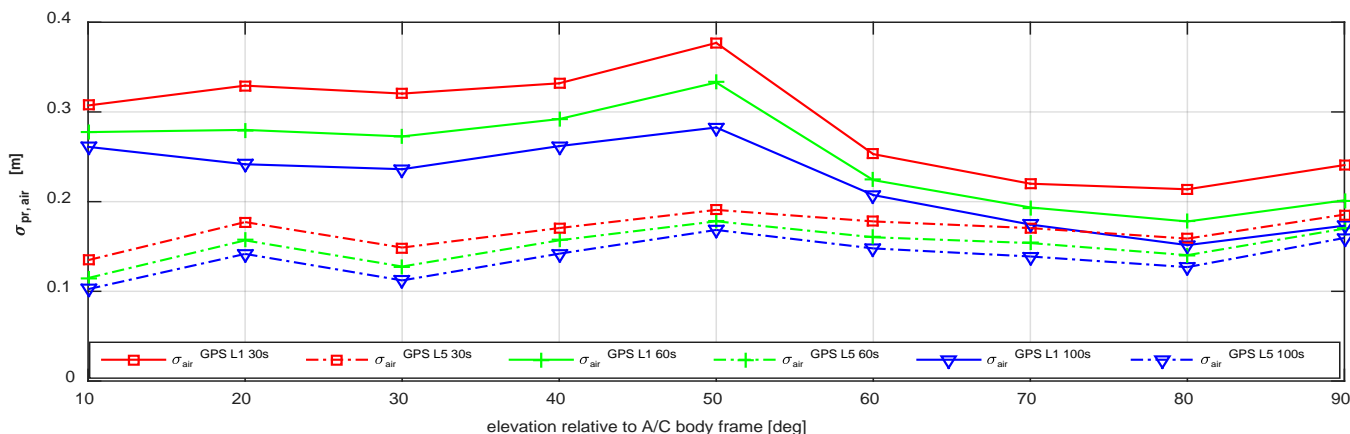


Figure 9 - $\sigma_{pr,air}$ versus elevation for GPS L5 (dashed lines) and GPS L1 (solid lines) for different smoothing constants: red(o) (30 s), green(+) (60 s), blue(v) (100 s)

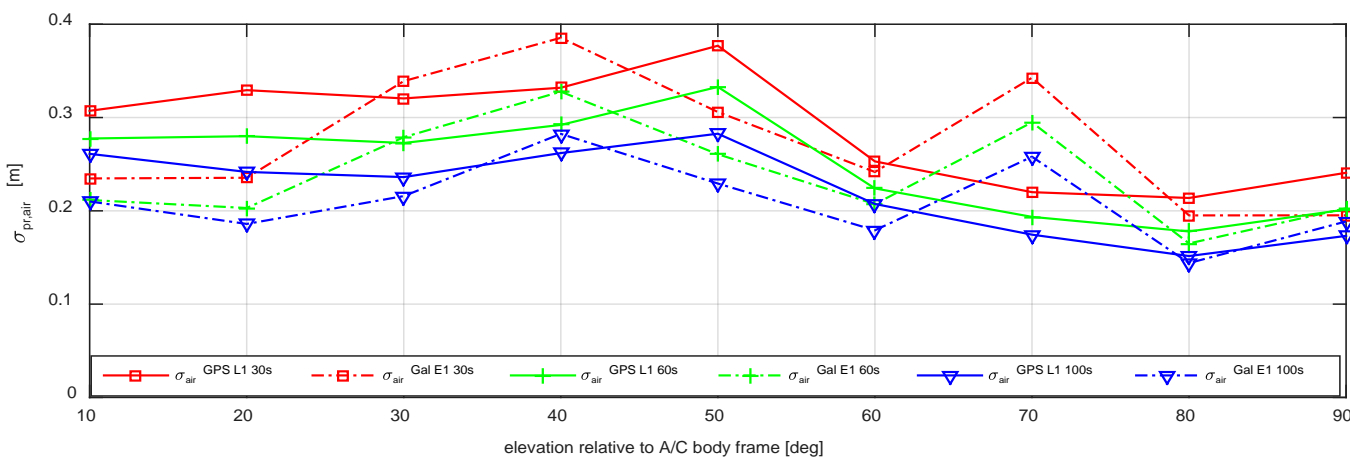


Figure 10 - $\sigma_{pr,air}$ versus elevation for Galileo E1 (dashed lines) and GPS L1 (solid lines) for different smoothing constants: red(o) (30 s), green(+) (60 s), blue(v) (100 s)

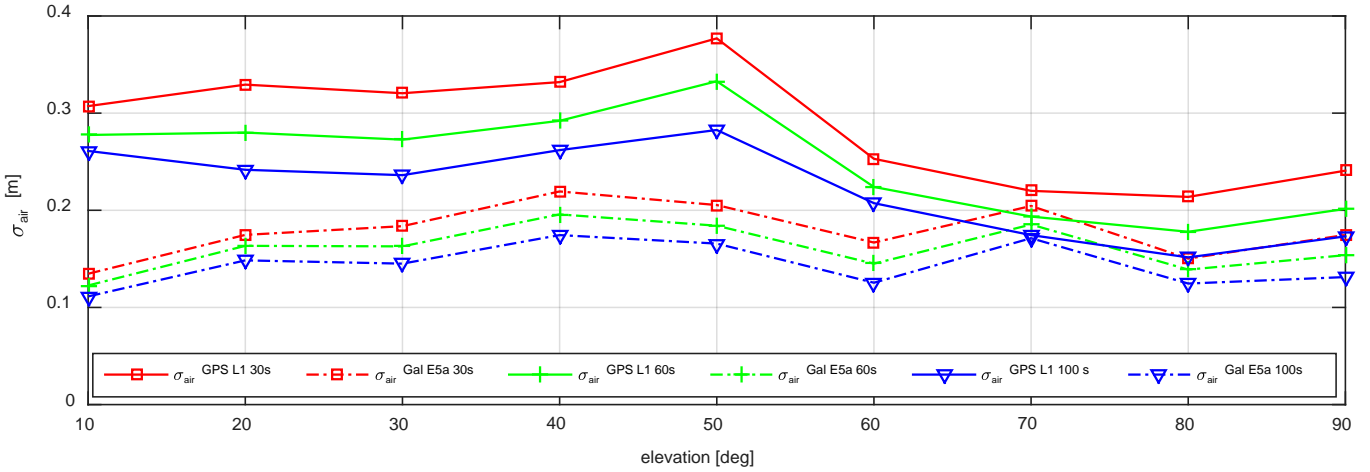


Figure 11 - σ_{pr_air} versus elevation for Galileo E5a (dashed lines) and GPS L1 (solid lines) for different smoothing constants: red(o) (30 s), green(+) (60 s), blue(v) (100 s)

The advantage of lower noise and multipath on L5 and E5a could bring improved performance to a future dual-frequency dual-constellation GBAS. In [6], a first concept for a dual-frequency dual-constellation is presented, taking into consideration the system-level benefits of this improved signal performance.

If a second frequency is continuously available in GBAS, an ionospheric free (Ifree) combination can be used in case of ionospheric disturbances. The disadvantage of the Ifree solution is the increased noise due to the combination of two code measurements [2]. Figure 12 shows σ_{pr_air} for the GPS Ifree L1/L5 combination with 100 seconds of smoothing compared with GPS L1 with 30 seconds of smoothing, as currently used in CAT III GBAS (GAST-D) [5]. For low elevations, the ratio of the increase of the error in the Ifree solution reaches values of 2.0 and decreases for high elevations to values of 1.7.

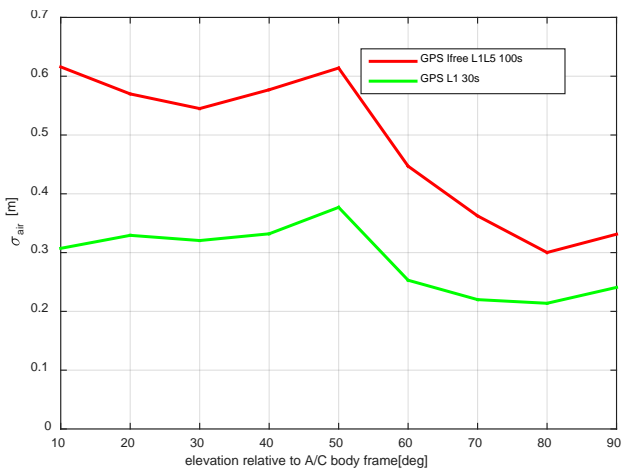


Figure 12 - σ_{pr_air} function of elevation for GPS Ifree combination (L1 and L5) 100 second smoothing (red curve) and GPS L1 30 seconds (green curve)

10. GROUND INFLUENCE

In the results presented in the previous sections, only the epochs in which the aircraft was at least 200 meters above ground level were considered. During flight at altitude, airborne multipath only results from reflections from the airframe, as discussed previously. However, additional multipath is expected when the aircraft approaches the ground and rolls out along the runway. Figure 13 shows a comparison of σ_{pr_air} curves for the altitudes above ground compared with those during approach and ground taxiing (below 200 meters).

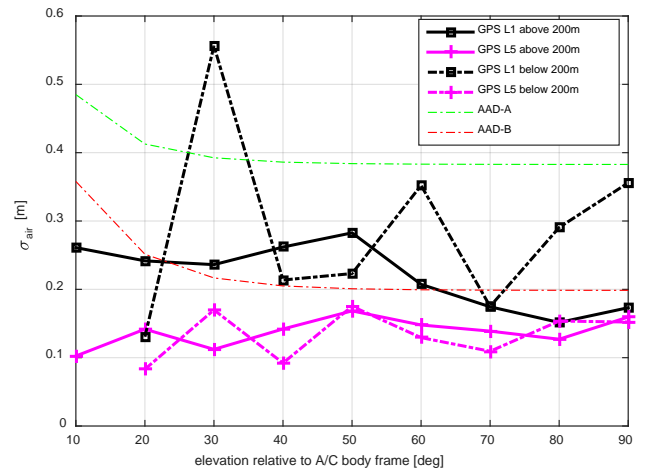


Figure 13 - σ_{pr_air} function of elevation for altitudes above 200 m (solid lines) and below 200 m (dashed line) for GPS L1 (black) and GPS L5 (magenta)

The solid lines represent the curves for high altitudes (above 200 meters) and the dashed ones for the low altitudes (below 200 meters). Measurements from the A320 were used to compute the curves with correlator spacings of 0.1 chips for L1/E1 and 1 chip for L5/E5a. Due to the limited amount of data for Galileo at lower

altitudes, only the GPS L1/L5 comparison is shown. It can be observed that the values of σ_{pr_air} near the ground are slightly larger than at higher altitudes. Again, the effect is more pronounced on L1 signals than on L5 ones, due to the better rejection of multipath on L5.

To further investigate the effects of ground reflections, we conducted additional data collections while removing the factor of airframe multipath. A small UAV, whose multipath from the airframe is very low compared to a manned aircraft, was used for these additional flight tests. As mentioned in Section 5, the UAV was used to collect data at an altitude of 20 meters and 0 meters (on the ground), while the KAIST IMT antenna mount (with virtually no airborne multipath contribution) was used to collect data at 10 meters.

Figure 14 shows the σ_{pr_air} curves for GPS L1 and Galileo E1 signals at three different altitudes. The square-solid lines represent the curves for GPS L1, while the circle-dashed lines indicate Galileo E1. The data was collected with a correlator spacing of 0.1 chips for L1/E1 and smoothed using a 100-second smoothing time constant. As shown in the figure, multipath due to ground reflections for GPS L1 and Galileo E1 decreased significantly with an increase in altitude. At low elevations with an altitude of 0 meters, Galileo E1 showed significantly better performance than GPS L1. This is because Galileo E1 is more efficient at rejecting long-delay multipath than GPS L1. At all altitudes, Galileo E1 performs better than GPS L1 in these results. However, the difference in σ_{pr_air} between L1 and E1 becomes less evident at higher altitudes, where the value of σ_{pr_air} itself due to ground multipath becomes relatively small.

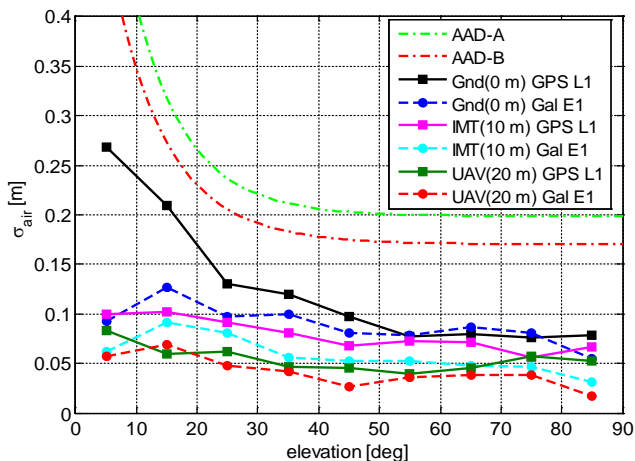


Figure 14 - σ_{pr_air} function of elevation for GPS L1 (solid lines) and Galileo E1 (dashed lines) for different altitudes; 0 m GPS L1 (black), 0 m Galileo E1 (blue), 10 m GPS L1 (magenta), 10 m Galileo E1 (cyan), 20 m GPS L1 (green), and 20 m Galileo E1 (red)

11. CONCLUSIONS

In this paper, we have provided the first evaluation of airborne multipath for GPS L1, L5 and Galileo E1 and E5a signals in a local-area differential context. Even though the results are preliminary, they show improved performance of the new signals, GPS L5 and Galileo E5a. Unlike the ground evaluations, Galileo E1 shows similar performance as GPS L1 due to the short-range behavior of airborne multipath reflections due to airframe geometry.

Several different contributors to the error represented by σ_{pr_air} have been investigated and discussed. Key receiver parameters are the receiver code correlator spacing and the related receiver front-end bandwidth. It has been shown that there is a large difference between a narrow and a wide value of the correlator spacing. For future multi-frequency multi constellation GBAS standards, the number of combinations of correlator spacing and receiver bandwidth should be restricted. This would also improve inter-frequency bias estimation, as it is strictly dependent on receiver parameters.

Another important contributor to the airborne multipath is the shape of the airframe itself and the location of the GNSS antenna with respect to airframe reflecting surfaces. This effect is more pronounced on the GPS L1 signals compared with the L5/E5a signals, as the L5 and E5a signals show better performance in terms of multipath rejection.

As observed on the ground measurements, the impact of the smoothing filter time constant is lower for GPS L5/Galileo E5a compared to GPS L1. However, the effectiveness of the smoothing filter is more pronounced on airborne measurements when compared to those from the ground, as airborne measurements are characterized by higher uncorrelated noise and slightly-correlated multipath.

The improved performance of GPS L5 and Galileo E5a signals demonstrated here would provide additional advantages to future multi-frequency multi-constellation GBAS systems now being considered (see [6]). In addition to contributing further geometric and signal diversity, the combined use of L1 and L5 (or E1 and E5a) can remove the anomalous ionospheric effects that create difficulties for today's single-frequency GBAS. Once L5 and E5a signals become standard on all GNSS satellites, they can take over the role as the primary signals within GBAS, allowing users to fully take advantage of their lower noise and multipath errors.

REFERENCES

- [1] Booth J., et al., *Validation of the Airframe Multipath Error Allocation for Local Area Differential GPS*, Proc. of ION ANNUAL MEETING, 26-28 June 2000, San Diego, CA, USA
- [2] Circiu M.-S., et al., *Evaluation of dual frequency GBAS Performance using flight data*, Proc. ION ITM, January 2014, San Diego, CA, USA
- [3] Circiu M.-S., et al., *Evaluation of GPS L5 and Galileo E1 and E5a Performance for Future Multi Frequency and Multi Constellation GBAS*, Proc. ION ITM 2015, January 2015, Dana Point, CA, USA
- [4] Eurocae ED-114A, "*Minimum operational performance specification for global navigation satellite ground based augmentation system ground equipment to support category I operations*", France, 2013
- [5] Felux M., et al., "*Towards Full GAST-D Capability – Flight Testing using the DLR's Experimental GBAS Station*", Proceedings of ION International Technical Meeting, January 2012, New Port Beach, CA,
- [6] Felux M., et al. - *Concept for a Dual Frequency Dual Constellation GBAS*, Proc. of the ION GNSS+ 2015, September 2015, Tampa, FL, USA
- [7] Hwang P., et al, (1999) "Enhanced Differential GPS Carrier-Smoothed Code Processing Using Dual-Frequency Measurements," Navigation, J. of the Inst. of Navigation, Vol. 46, No. 2
- [8] Kim M., Kim K., Lee J., Pullen S., "High Integrity GNSS Navigation and Safe Separation Distance to Support Local-Area UAV networks," Proc. of ION GNSS 2014, September 2014, Tampa, FL, USA
- [9] McGraw G.-A., et al., "Development of the LAAS Accuracy Models", Proc. of ION GPS 2000, September 2000, Salt Lake City, UT, USA
- [10] Murphy T., Harris M., Booth J., Geren P., Pankaskie T., Clark B., Burns J., Urda T.– Results from the program for the investigation of airborne multipath errors, Proc. of ION NTM, 24-26 January 2005, San Diego, CA, USA
- [11] Murphy T., Harris M., Geren P., Pankaskie T., Clark B., Burns J., – *More results from the investigation of airborne multipath errors*, Proc. of ION ITM, 13016 September 2005, Long Beach, CA, USA
- [12] RTCA DO-253C (2008), *Minimum operational performance standards for GPS local area augmentation system airborne equipment*, December 2008, Washington